Mixed-metal cluster chemistry VII: some phosphine and alkyne chemistry of $Cp_2Mo_2Ir_2(CO)_{10}$; X-ray crystal structures of $Cp_2Mo_2Ir_2(\mu\text{-}CO)_3(CO)_6(PMe_3)$ and $Cp_2Mo_2Ir_2(\mu_4\text{-}\eta^2\text{-}HC_2Ph)(\mu\text{-}CO)_4(CO)_4$

N.T. Lucas [a], M.G. Humphrey [a,*], P.C. Healy [b], M.L. Williams [b]

[a] *Department of Chemistry, Australian National University, Canberra, ACT 0200, Australia*
[b] *Faculty of Science and Technology, Griffith University, Nathan, Qld 4111, Australia*

Abstract

Reactions of $Cp_2Mo_2Ir_2(CO)_{10}$ (1) with stoichiometric amounts of phosphines afforded the substitution products $Cp_2Mo_2Ir_2(CO)_{10-x}L_x$ (L = PPh_3, x = 1 (5), 2 (6); L = PMe_3, x = 1 (7), 2 (8)), in fair to excellent yields (36–78%), shown by low temperature ^{31}P NMR to consist of mixtures of interconverting isomers. An X-ray structural study of $Cp_2Mo_2Ir_2(\mu\text{-}CO)_3(CO)_6(PMe_3)$ (7a), one isomer of 7, revealed that the PMe_3 ligand occupies the electronically-preferred axial site (with respect to the plane of the bridging carbonyls). Geometries of all other isomers of 5–8 have been postulated from a combination of NMR data and results from the analogous $Cp_2W_2Ir_2(CO)_{10}$ system. Reactions of 1 with a range of alkynes afforded $Cp_2Mo_2Ir_2(\mu_4\text{-}\eta^2\text{-}RC_2R')(CO)_8$ (R = R' = Ph (9), H (14); R = H, R' = Ph (10), 4-$C_6H_4NO_2$ (11), 4,4'-$C_6H_4C\equiv CC_6H_4NO_2$ (12), CH_2Br (13)) in fair to good yields (34–80%). An X-ray structural study of 10 revealed that the alkynes have formally inserted into the Mo–Mo bond of 1, to afford clusters with a pseudooctahedral core geometry. Qualitative analysis of reaction rates for the syntheses of 9–14 revealed the trends acetylene > terminal alkyne > internal alkyne and 4-nitrophenylacetylene > phenylacetylene, assigned to a combination of electronic and steric effects. © 1997 Elsevier Science S.A.

Keywords: Molybdenum; Iridium; Carbonyl; Cyclopentadienyl; Cluster; Phosphine; Alkyne; Acetylene; Crystal structure

1. Introduction

The chemistry of mixed-metal clusters continues to be of interest, driven to some extent by the possibility of exploiting the polar metal-metal bonds in unusual and/or enhanced substrate activation. The varying constituent metals of the cluster core also afford the possibility of probing metallo-, bond- and site-selectivity for a variety of reagents. We recently reported the high-yielding synthesis and structural characterization of the tetrahedral cluster $Cp_2Mo_2Ir_2(CO)_{10}$ (1) [2]; together with $Ir_4(CO)_{12}$ (2) and $CpMoIr_3(CO)_{11}$ (3), it completes a set of three isostructural clusters related by sequential (conceptual) isolobal replacement of cluster core vertices, of obvious interest for probing metallo-, bond- and site-selectivity of reactions. The chemistry of 2 with

phosphines and alkynes has been reported in depth [3], and we have recently carried out a study of the phosphine reaction chemistry of 3 [1]. We report herein the results of reacting 1 with the phosphines PPh_3 and PMe_3, and with a range of alkynes, together with comparison to the related phosphine and alkyne chemistry of 3 and $Cp_2W_2Ir_2(CO)_{10}$ (4), the heavier homologue of 1.

2. Results and discussion

2.1. Syntheses and characterization of $Cp_2Mo_2Ir_2(CO)_{10-x}L_x$ (L = PPh_3, x = 1 (5), 2 (6); L = PMe_3, x = 1 (7), 2 (8))

The reactions of $Cp_2Mo_2Ir_2(CO)_{10}$ (1) with x equivalents of PPh_3 (x = 1 or 2) proceeded in dichloromethane at room temperature (Scheme 1). Re-

* Corresponding author. Tel.: +61 6 2492927; Fax: +61 6 2490760; e-mail: Mark.Humphrey@anu.edu.au

action with one equivalent afforded the mono-substituted cluster $Cp_2Mo_2Ir_2(CO)_9(PPh_3)$ (5) in good yield, but with some unsubstituted and bis-substituted cluster as minor products. Similarly, reaction with 2 equivalents of PPh_3 under the same conditions afforded the bis-substituted cluster $Cp_2Mo_2Ir_2(CO)_8(PPh_3)_2$ (6) as the major product, but with a significant quantity of mono-substituted cluster. Work-up of the latter reaction revealed decomposition of the bis-substituted cluster on the thin-layer chromatographic plate to afford the mono-substituted product. There was no evidence for tris-substitution of 1.

The two substitution products were characterized by a combination of IR, ^{1}H- and ^{31}P-NMR spectroscopy, MS and microanalyses (for 5; 6 decomposed slowly at room temperature to afford 5, and attempts to isolate it in a pure form were unsuccessful). The solution IR spectra contain ν(CO) bands in the bridging as well as terminal carbonyl regions with the number of bands in the spectra of 5 indicative of the presence of isomers in solution. The ^{1}H-NMR spectra contain resonances in the phenyl and cyclopentadienyl regions in the expected ratios. The mass spectra contain molecular ions and fragment ions corresponding to sequential loss of all carbonyl ligands. Fragmentation by loss of phosphine ligands from 6 is competitive with loss of carbonyl ligands for $[M-2CO]^+$.
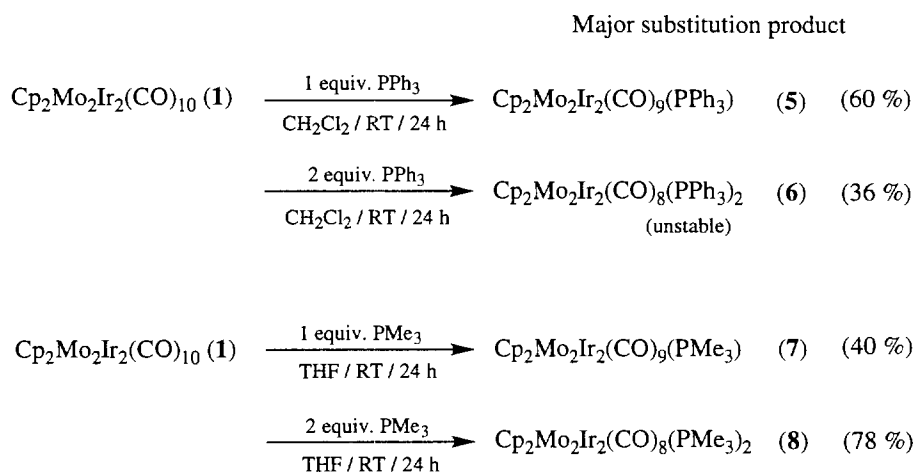
The reactions of 1 with x equivalents of PMe_3 ($x = 1$, 2 or excess) proceeded in tetrahydrofuran at room temperature (Scheme 1). Reactions of one or two equivalents afforded the expected mono- or bis-substituted cluster as the major products respectively, but with some contamination similar to that found with PPh_3. The reaction of excess PMe_3 afforded the bis-substituted cluster as the sole product. The clusters $Cp_2Mo_2Ir_2(CO)_9(PMe_3)$ (7) and $Cp_2Mo_2Ir_2(CO)_8(PMe_3)_2$ (8) were characterized by IR, ^{1}H- and ^{31}P-NMR spectroscopy, MS, microanalyses

and, for one isomer of 7, a single crystal X-ray diffraction study. Edge-bridging carbonyl ligands are observed in the solution IR spectra of both substituted complexes; as seen with the PPh_3-substituted cluster 5, the number of bands in the ν(CO) region are consistent with the presence of isomers. The ^{1}H-NMR spectra contain resonances in the cyclopentadienyl and methyl regions in the expected ratios. The mass spectra contain molecular ions at the predicted values with fragmentation by loss of PMe_3 or methyl becoming increasingly competitive with loss of carbonyl on moving from 7 to the more highly substituted complex 8. Phosphines are lost preferentially to the cyclopentadienyl groups; loss of cyclopentadienyl occurs only after all phosphines are removed.

2.2. X-ray structural study of $Cp_2Mo_2Ir_2(\mu-CO)_3(CO)_6(PMe_3)$ (7a)

An isomer of 7, namely 7a, was subjected to X-ray diffraction analysis; the solid state molecular structure of $Cp_2Mo_2Ir_2(\mu-CO)_3(CO)_6(PMe_3)$ (7a) as determined by single crystal X-ray study is consistent with the formulation above, defines the substitution site of the phosphine in this isomer, and facilitates interpretation of the ^{31}P-NMR spectra. Atomic coordinates are given in Table 1 and selected interatomic bond lengths and angles are listed in Table 2. Fig. 1 contains an ORTEP plot of 7a, showing the molecular structure and atomic labelling scheme.

The cluster has the closed pseudotetrahedral Mo_2Ir_2 core geometry of the precursor cluster 1 [2]. Each molybdenum atom bears one η^5-cyclopentadienyl group; 3 bridging carbonyls span a $MoIr_2$ face with another 6 carbonyls in terminal modes distributed over the cluster core. An iridium-ligated trimethylphosphine completes the coordination sphere to give an electron precise cluster with 60 CVE ($2 \times 6(Mo) + 2 \times 9(Ir) + 2 \times$

Major substitution product

$Cp_2Mo_2Ir_2(CO)_{10}$ (1) $\xrightarrow[\text{CH}_2\text{Cl}_2 \text{ / RT / 24 h}]{\text{1 equiv. PPh}_3}$ $Cp_2Mo_2Ir_2(CO)_9(PPh_3)$ (5) (60 %)

$\xrightarrow[\text{CH}_2\text{Cl}_2 \text{ / RT / 24 h}]{\text{2 equiv. PPh}_3}$ $Cp_2Mo_2Ir_2(CO)_8(PPh_3)_2$ (6) (36 %)

(unstable)

$Cp_2Mo_2Ir_2(CO)_{10}$ (1) $\xrightarrow[\text{THF / RT / 24 h}]{\text{1 equiv. PMe}_3}$ $Cp_2Mo_2Ir_2(CO)_9(PMe_3)$ (7) (40 %)

$\xrightarrow[\text{THF / RT / 24 h}]{\text{2 equiv. PMe}_3}$ $Cp_2Mo_2Ir_2(CO)_8(PMe_3)_2$ (8) (78 %)

Scheme 1.

5(Cp) + 9 × 2(CO) + 2(PMe$_3$)). The Ir(1)–Ir(2) distance (2.697(1) Å) is similar to that seen in **1** (2.697(1) Å) and marginally shorter than that in Cp$_2$W$_2$Ir$_2$(CO)$_{10}$ (2.722(1) Å). The Mo–Ir core bond distances increase slightly on substitution of CO by PMe$_3$ (Mo–Ir$_{av}$ 2.8793 Å in **7a** compared to Mo–Ir$_{av}$ 2.857 Å for **1**). The Mo–Mo vector in **7a** (3.094(2) Å) is shortened slightly compared to that in **1** (3.112(1) Å). Intracore bond angles are all close to 60° as expected. As was observed with **1**, angles centred at iridium for **7a** are slightly larger (61.263(10)–65.53(2)°) than those centred at molybdenum (55.701(4)–58.031(5)°). The carbonyls CO(12), CO(13) and CO(23) are in edge bridging sites about the metal–metal vectors in the Ir(1)Ir(2)Mo(3) plane; CO(31) adopts a semi-bridging geometry, with C(31) · · · Mo(4) 2.8401(6) Å. Curtis et al. have defined an asymmetry parameter, α, to evaluate semi-bridging character [4,5]. For Mo(3)–C(31) · · · Mo(4), $\alpha = 0.48$, which falls within the $0.1 < \alpha < 0.6$ 'semi-bridging'

Table 1
Non-hydrogen atom coordinates and equivalent isotropic displacement parameters for **7a**

Atom	x	y	z	B_{eq}
Ir(1)	0.06372(7)	0.32647(5)	0.41618(8)	2.35(2)
Ir(2)	0.21251(7)	0.18432(5)	0.36844(8)	2.29(2)
Mo(3)	0.2455(1)	0.3454(1)	0.1971(2)	2.26(3)
Mo(4)	−0.0221(1)	0.2193(1)	0.1391(2)	2.31(3)
P(1)	0.4017(5)	0.1858(4)	0.5611(6)	3.2(1)
O(11)	−0.220(1)	0.351(1)	0.503(2)	6.6(5)
O(12)	0.037(1)	0.1627(10)	0.624(1)	4.0(4)
O(13)	0.006(1)	0.4790(10)	0.194(1)	4.1(4)
O(14)	0.231(1)	0.458(1)	0.652(1)	4.1(4)
O(22)	0.215(2)	−0.016(1)	0.320(2)	5.3(4)
O(23)	0.407(1)	0.175(1)	0.134(1)	4.5(4)
O(31)	0.156(1)	0.304(1)	−0.147(1)	4.5(4)
O(41)	−0.127(1)	0.064(1)	0.332(2)	5.1(4)
O(42)	0.119(1)	0.069(1)	−0.029(2)	4.5(4)
C(11)	−0.117(3)	0.345(2)	0.475(2)	6.0(7)
C(12)	0.083(2)	0.201(1)	0.528(2)	3.0(5)
C(13)	0.067(2)	0.415(1)	0.236(2)	2.8(4)
C(14)	0.167(2)	0.408(1)	0.569(2)	3.1(5)
C(22)	0.214(2)	0.069(2)	0.349(2)	4.2(5)
C(23)	0.328(2)	0.218(1)	0.193(2)	2.6(4)
C(31)	0.171(2)	0.312(1)	−0.015(2)	3.2(5)
C(41)	−0.083(2)	0.120(1)	0.268(2)	3.4(5)
C(42)	0.074(2)	0.124(1)	0.037(2)	2.5(4)
C(211)	0.460(2)	0.290(2)	0.668(2)	4.8(6)
C(212)	0.557(2)	0.149(2)	0.496(2)	5.6(7)
C(213)	0.378(2)	0.105(2)	0.708(2)	5.2(6)
C(301)	0.439(2)	0.396(2)	0.104(2)	4.3(6)
C(302)	0.349(2)	0.463(2)	0.085(3)	5.1(7)
C(303)	0.326(2)	0.498(2)	0.220(3)	4.6(6)
C(304)	0.403(2)	0.456(2)	0.335(2)	4.5(6)
C(305)	0.476(2)	0.392(2)	0.267(3)	5.0(6)
C(401)	−0.133(2)	0.319(2)	−0.041(2)	3.5(5)
C(402)	−0.140(2)	0.230(2)	−0.107(2)	4.4(6)
C(403)	−0.219(2)	0.173(1)	−0.026(2)	3.6(5)
C(404)	−0.261(2)	0.224(2)	0.095(2)	4.5(6)
C(405)	−0.206(2)	0.318(2)	0.084(2)	4.0(5)

Table 2
Selected bond lengths (Å) and angles (°) for **7a**

Ir(1)–Ir(2)	2.697(1)	Mo(3)–C(301)	2.29(2)
Ir(1)–Mo(3)	2.852(2)	Mo(3)–C(302)	2.29(2)
Ir(1)–Mo(4)	2.864(2)	Mo(3)–C(303)	2.33(2)
Ir(2)–Mo(3)	2.892(2)	Mo(3)–C(304)	2.36(2)
Ir(2)–Mo(4)	2.909(2)	Mo(3)–C(305)	2.31(2)
Mo(3)–Mo(4)	2.094(2)	Mo(4)–C(401)	2.39(2)
Ir(2)–P(1)	2.317(5)	Mo(4)–C(402)	2.32(2)
Ir(1)–C(12)	2.13(2)	Mo(4)–C(403)	2.29(2)
Ir(2)–C(12)	2.07(2)	Mo(4)–C(404)	2.33(1)
Ir(1)–C(13)	2.11(2)	Mo(4)–C(405)	2.39(2)
Mo(3)–C(13)	2.16(2)	C(12)–O(12)	1.18(2)
Ir(2)–C(23)	2.12(2)	C(13)–O(13)	1.18(2)
Mo(3)–C(23)	2.10(2)	C(23)–O(23)	1.21(2)
Ir(1)–C(11)	1.96(2)	C(11)–O(11)	1.09(2)
Ir(1)–C(14)	1.90(2)	C(14)–O(14)	1.13(2)
Ir(2)–C(22)	1.71(3)	C(22)–O(22)	1.28(3)
Mo(3)–C(31)	1.94(2)	C(31)–O(31)	1.16(2)
Mo(4)–C(41)	2.01(2)	C(41)–O(41)	1.12(2)
Mo(4)–C(42)	2.01(1)	C(42)–O(42)	1.14(2)
Ir(2)–Ir(1)–Mo(3)	62.74(1)	Ir(2)–C(23)–Mo(3)	87.05(1)
Ir(2)–Ir(1)–Mo(4)	62.99(1)	Ir(1)–C(11)–O(11)	174.126(2)
Mo(3)–Ir(1)–Mo(4)	65.53(2)	Ir(1)–C(14)–O(14)	174.8644(2)
Ir(1)–Ir(2)–Mo(3)	61.263(10)	Ir(2)–C(22)–O(22)	174.2578(7)
Ir(1)–Ir(2)–Mo(4)	61.31(1)	Mo(3)–C(31)–O(31)	162.872(5)
Mo(3)–Ir(2)–Mo(4)	64.46(1)	Mo(4)–C(41)–O(41)	174.632(2)
Ir(1)–Mo(3)–Ir(2)	55.997(4)	Mo(4)–C(42)–O(42)	174.9123(8)
Ir(1)–Mo(3)–Mo(4)	57.41(2)	Ir(1)–C(12)–O(12)	138.453(9)
Ir(2)–Mo(3)–Mo(4)	58.031(5)	Ir(2)–C(12)–O(12)	140.814(5)
Ir(1)–Mo(4)–Ir(2)	55.701(4)	Ir(1)–C(13)–O(13)	135.401(9)
Ir(1)–Mo(4)–Mo(3)	57.059(3)	Mo(3)–C(13)–O(13)	139.681(5)
Ir(2)–Mo(4)–Mo(3)	57.51(2)	Ir(2)–C(23)–O(23)	130.745(10)
Ir(1)–C(12)–Ir(2)	80.550(7)	Mo(3)–C(23)–O(23)	142.137(3)
Ir(1)–C(13)–Mo(3)	84.300(5)		

regime. The remaining 5 carbonyl ligands are terminal. The Ir–P distance (2.317(5) Å) and intraphosphine bond lengths and angles are not unusual. With respect to the
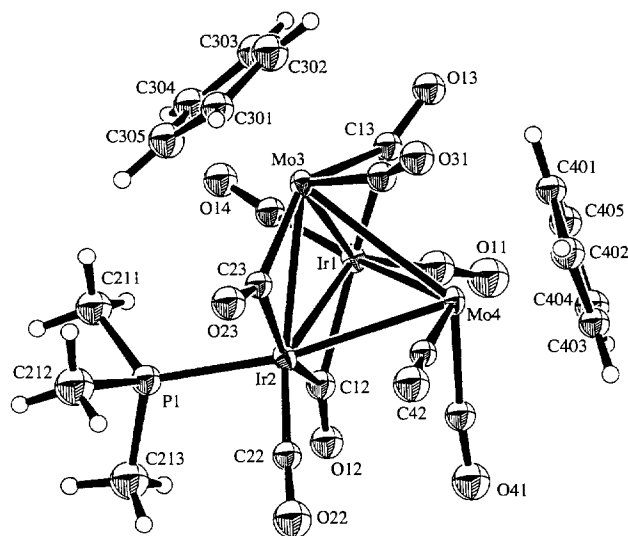

Fig. 1. Molecular structure and atomic labelling scheme for **7a**. Thermal envelopes of 50% probability are shown for the non-hydrogen atoms; hydrogen atoms have arbitrary radii of 0.1 Å.

Table 3
^{31}P-NMR data for **5–8** ($Cp_2Mo_2Ir_2(\mu\text{-}CO)_3(CO)_{7-x}(L)_x$, (L = PPh_3, PMe_3; x = 1 or 2) (230 K)

	Complex	^{31}P-NMR chemical shifts (ppm)[a]	Suggested sites/s for L substitution, with respect to (μ-CO_3 plane	isomer ratio
x = 1, L = PPh_3	**5a**	14.9	axial[b]	1
	5b	3.2	apical	2
x = 2, L = PPh_3	**6**	18.4, 13.5 (1:1)	radial, axial	
x = 1, L = PMe_3	**7a**	−21.9	axial[c,d]	f
	7b	−22.8	axial[e]	f
x = 2, L = PMe_3	**8a**	−17.2, −34.3 (1:1)	radial, apical	8
	8b	−22.0, −27.0 (1:1)	axial, apical	2

[a] $CDCl_3$.
[b] Crystallographically confirmed for the tungsten analogue $Cp_2W_2Ir_2(\mu\text{-}CO)_3(CO)_6(PPh_3)$ [5].
[c] Crystallographically confirmed (this work).
[d] Cp groups (axial, apical).
[e] Cp groups (radial, apical).
[f] Not deconvolutable.

5a
$Cp_2Mo_2Ir_2(\mu\text{-}CO)_3(CO)_6(PPh_3)$

5b
$Cp_2Mo_2Ir_2(\mu\text{-}CO)_3(CO)_6(PPh_3)$

6
$Cp_2Mo_2Ir_2(\mu\text{-}CO)_3(CO)_5(PPh_3)_2$

7a
$Cp_2Mo_2Ir_2(\mu\text{-}CO)_3(CO)_6(PMe_3)$

7b
$Cp_2Mo_2Ir_2(\mu\text{-}CO)_3(CO)_6(PMe_3)$

8a
$Cp_2Mo_2Ir_2(\mu\text{-}CO)_3(CO)_5(PMe_3)_2$

8b
$Cp_2Mo_2Ir_2(\mu\text{-}CO)_3(CO)_5(PMe_3)_2$
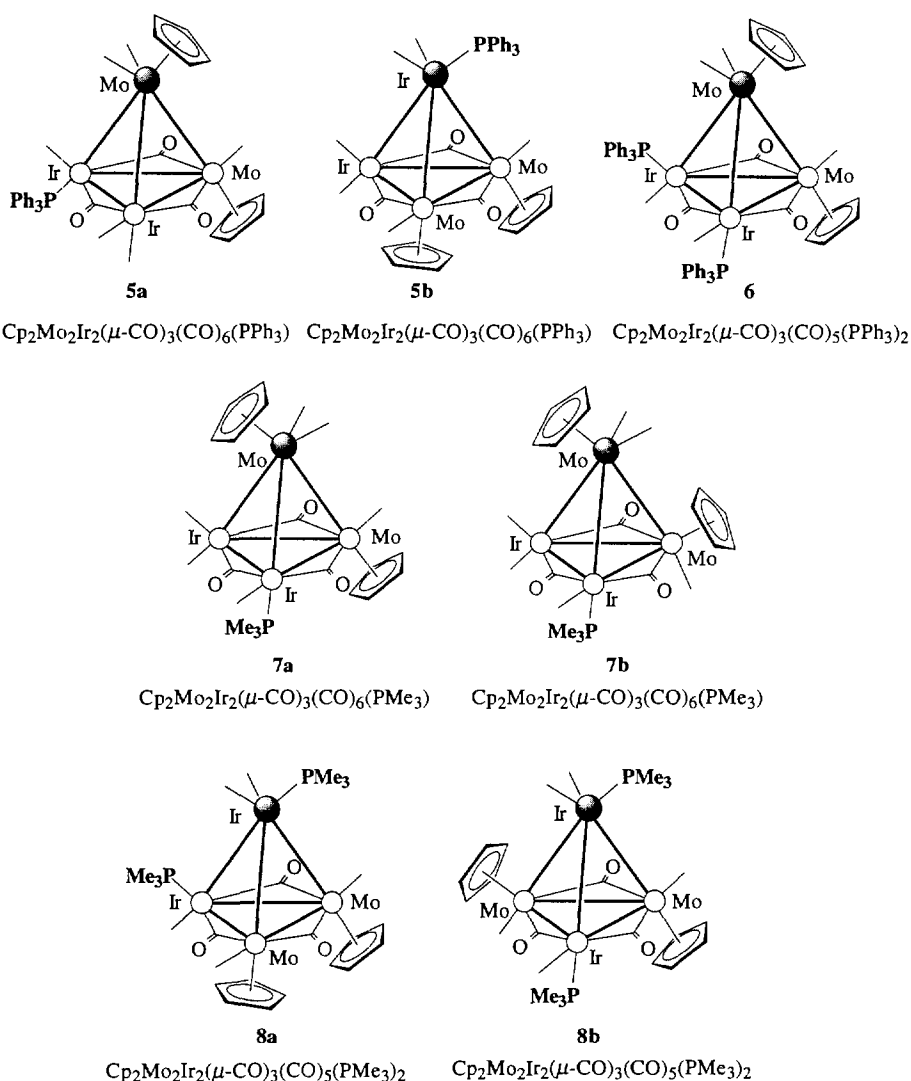
Fig. 2. Suggested configurations for **5–8**.

plane of bridging carbonyls, PMe$_3$ occupies an axial coordination site with the cyclopentadienyl groups in axial and apical positions.
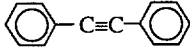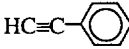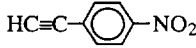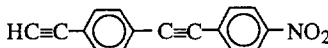
2.3. Suggested isomer assignment

The presence of isomers for the phosphine substituted derivatives of 1 is indicated by the number of bands observed in the IR spectra and (in some cases) multiple resonances in the ^{31}P-NMR spectra. ^{31}P-NMR spectra of these compounds at room temperature show substantial broadening due to CO fluxional processes. Isomers may arise from differing ligand sites (phosphines and cyclopentadienyl groups), or from variations in the location of the plane of bridging carbonyls (although bridging around a Mo$_2$Ir face may be sterically unfavourable). Substitution sites for the Cp$_2$Mo$_2$Ir$_2$(CO)$_{10-n}$(L)$_n$ system have been assigned from (a) crystallographically-verified isomers in the dimolybdenum–diiridium and ditungsten–diiridium systems, (b) the substitution pattern in the tetrairidium and molybdenum–triiridium systems, and (c) chemical shifts in the ^{31}P-NMR spectra (for the tungsten–triiridium system, the chemical shift sequence radial > axial > apical was observed [6]). Results of these studies in the dimolybdenum–diiridium system are summarized in Table 3. Suggested geometries for the isomers are indicated in Fig. 2.

Axial-ligated triphenylphosphine is observed at 14.9 ppm, whereas apical-ligated triphenylphosphine is found at 3.2 ppm for the mono-substituted cluster. The isomer

proposed for the bis-substituted cluster has radial and axial ligated phosphines with cyclopentadienyl groups in axial and apical sites, the most sterically favoured configuration for tetra-substitution. Radial-, axial- and apical-ligation at 1 is also observed for trimethylphosphine. The phosphine in 7a occupies an axial site (crystallographically characterized), with two close resonances in the ^{31}P-NMR spectrum proposed as corresponding to isomers with the cyclopentadienyl group in axial and radial positions. The bis-substituted product 8 displays two isomers in solution at 230 K, seen as pairs of sharp and broad resonances. The broad pair (which sharpen at 213 K) are believed to correspond to trimethylphosphine in radial and apical sites, the sharp pair to a axial, apical isomer. The cyclopentadienyl groups occupy the remaining sites so as to give the radial, diaxial, apical configuration, as was also observed for 6, the bis-triphenylphosphine substituted product. It is emphasized that these are suggested configurations based on available data — clearly further structural studies are required to corroborate these assignments. Although these possible geometries are consistent with the phosphine P chemical shift sequence, they require locating the plane of bridging carbonyls about a Mo$_2$Ir plane, a geometry for which there are thus far no structural precedents. It may be more favourable for the triphenylphosphine (cone angle 145°) than for the trimethylphosphine (cone angle 118°) derivatives for cyclopentadienyl ligands (cone angle 136°) to ligate iridiums in the bridging carbonyl plane, as this plane is the most
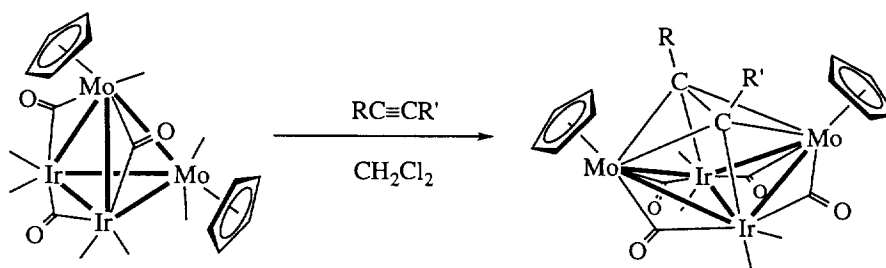
RC≡CR'	conditions	major product	(yield)
⬡–C≡C–⬡	reflux / 24 h	9	(80 %)
HC≡C–⬡	RT / 64 h	10	(61 %)
HC≡C–⬡–NO$_2$	RT / 20 h	11	(64 %)
HC≡C–⬡–C≡C–⬡–NO$_2$	RT / 50 h	12	(63 %)
HC≡CCH$_2$Br	RT / 20 h	13	(34 %)
HC≡CH	RT / 2 h	14	(44 %)

Scheme 2.

sterically cluttered; the phosphine will then occupy an apical site, a geometry postulated for **5b**.

2.4. Syntheses and characterization of $Cp_2Mo_2Ir_2(\mu_4$-η^2-$RC_2R')(CO)_8$

The cluster $Cp_2Mo_2Ir_2(CO)_{10}$ (**1**) and the internal alkyne diphenylacetylene were heated in refluxing dichloromethane until all starting material was consumed (24 h) (Scheme 2). Following preparative TLC and crystallization, dark green $Cp_2Mo_2Ir_2(\mu_2$-η^2-$PhC_2Ph)(CO)_8$ (**9**) was isolated in 80% yield, and characterized by IR, ^{1}H-NMR spectroscopy, MS and microanalyses. The solution IR spectrum has seven $\nu(CO)$ bands, four in the terminal carbonyl region and three in the bridging carbonyl region (one as a shoulder). The ^{1}H-NMR spectrum contains resonances in the phenyl and cyclopentadienyl regions in the ratio 1:1, with the singlet observed for the cyclopentadienyl resonance giving information about the symmetry of the complex. The mass spectrum contains a molecular ion and fragmentation corresponding to $[M-2CO]^+$ and then sequential loss of all carbonyl ligands.

The reaction of **1** with all of the terminal alkynes investigated proceeded at room temperature; the times for consumption of all starting cluster are given in Scheme 2. Following preparative chromatography and crystallization, $Cp_2Mo_2Ir_2(\mu_4$-η^2-$HC_2R)(CO)_8$ (R = Ph (**10**), 4-$C_6H_4NO_2$ (**11**), 4,4'-$C_6H_4C\equiv CC_6H_4NO_2$ (**12**), CH_2Br (**13**) and H (**14**)) were isolated in fair to good (34–64%) yield and characterized by IR, ^{1}H-NMR spectroscopy, MS and microanalyses. Some of these reactions afforded products in trace to minor amounts, the identities of which have not thus far been determined. Solution IR spectra for **10–14** contain four $\nu(CO)$ bands in the terminal carbonyl region and two broad bands in the bridging carbonyl region, with that for **12** containing a weak absorption at 2217 cm^{-1} corresponding to the uncomplexed internal alkyne linkage. The ^{1}H-NMR spectra for **10–14** contain a characteristic resonance in the range 10.22–9.23 ppm corresponding to the acetylenic proton(s), together with phenyl (where appropriate) and cyclopentadienyl resonances. The mass spectra of **10–12**, **14** show molecular ions, and fragmentation by sequential loss of all carbonyl ligands; the mass spectrum of **13** contains no molecular ion, and reveals that loss of one cyclopentadienyl ligand occurs preferentially to loss of carbonyl, the result perhaps of the close proximity of the bromine to the cyclopentadienyl groups assisting loss of one of these rings. The identity of **10** was confirmed by a X-ray crystallographic study.

2.5. X-ray structural study of $Cp_2Mo_2Ir_2(\mu_4$-η^2-$HC_2Ph)(\mu$-$CO)_4(CO)_4$ (10)

A single crystal X-ray diffraction study of $Cp_2Mo_2Ir_2(\mu_4$-η^2-$HC_2Ph)(\mu$-$CO)_4(CO)_4$ (**10**) was un-

dertaken and confirms the expected molecular composition. Atomic coordinates are given in Table 4 and selected bond lengths and angles are displayed in Table 5. Fig. 3 contains an ORTEP plot of **10** showing the molecular structure and atomic labelling scheme.

The cluster **10** possesses a Mo_2Ir_2 core in which the metals adopt a butterfly geometry: the iridium atoms form the hinge and the molybdenum atoms reside at the wing tips. Each molybdenum atom bears a cyclopentadienyl ring and each iridium is ligated by two terminal carbonyl ligands. The phenylacetylene ligand bridges all four metals in a μ_4-η^2-fashion, lying parallel to the $Ir(1)-Ir(2)$ vector and completing a *closo*-octahedral core consisting of the four metals and the two 'acetylenic' carbon atoms. The Ir–Ir bond length

Table 4
Non-hydrogen atom coordinates and equivalent isotropic displacement parameters for **10**

Atom	x	y	z	B_{eq}
Ir(1)	0.10140(3)	0.13025(4)	0.82628(2)	2.811(9)
Ir(2)	0.28268(3)	0.16147(4)	0.86163(2)	2.924(9)
Mo(1)	0.18987(6)	0.08706(8)	0.70892(4)	3.00(2)
Mo(2)	0.21188(6)	−0.03495(8)	0.93630(4)	2.87(2)
Cl(1)	0.5279(8)	0.445(1)	0.9004(7)	6.4(3)
Cl(3)	0.497(1)	0.547(1)	0.9608(8)	7.8(3)
O(1)	−0.0967(5)	0.0469(8)	0.7824(5)	6.7(3)
O(2)	0.0606(6)	0.4006(8)	0.8687(5)	6.7(3)
O(3)	0 4894(7)	0.169(1)	0.9124(8)	13.3(5)
O(4)	0.2706(7)	0.4390(8)	0.9106(5)	7.1(3)
O(5)	0 0247(6)	0.2682(8)	0.6662(4)	6.3(2)
O(6)	0.0648(5)	0.1116(7)	0.9906(4)	4.9(2)
O(7)	0.3055(6)	0.3331(7)	0.7221(4)	6.1(2)
O(8)	0.3480(6)	0.1481(9)	1.0462(4)	6.6(3)
C(1)	−0.0218(8)	0.075(1)	0.7975(6)	4 3(3)
C(2)	0.0758(7)	0.300(1)	0.8524(6)	3 9(3)
C(3)	0.4128(9)	0.164(1)	0.8912(7)	6.3(4)
C(4)	0.2764(8)	0.336(1)	0.8937(6)	4.4(3)
C(5)	0.0834(8)	0.200(1)	0.6988(6)	4.3(3)
C(6)	0.1125(7)	0.0748(9)	0 9541(5)	3.3(2)
C(7)	0.2662(8)	0.241(1)	0.7351(6)	4.4(3)
C(8)	0.2994(7)	0.097(1)	0.9923(6)	4.2(3)
C(9)	0.176(1)	0.135(1)	0.5816(6)	6.2(4)
C(10)	0.1101(10)	0.046(2)	0.5835(7)	5.9(4)
C(11)	0.152(1)	−0.064(1)	0.6102(7)	6.0(4)
C(12)	0.245(1)	−0.048(1)	0.6280(6)	5.3(3)
C(13)	0.2601(9)	0.078(1)	0.6093(6)	5.5(4)
C(14)	0.1393(7)	−0.182(1)	0.9933(6)	4.5(3)
C(15)	0.1857(10)	−0.250(1)	0.9494(6)	4.9(3)
C(16)	0.2802(10)	−0.231(1)	0.9808(7)	5.9(4)
C(17)	0.2913(8)	−0.151(1)	1.0447(7)	5.5(3)
C(18)	0.2061(9)	−0.120(1)	1.0529(6)	5.1(3)
C(19)	0.1583(6)	−0.0400(8)	0.8034(5)	2.3(2)
C(20)	0.2551(6)	−0.0265(8)	0.8201(4)	2.7(2)
C(21)	0.3160(7)	−0.1341(10)	0.8073(5)	3.2(2)
C(22)	0.2828(8)	−0.2558(9)	0.7858(6)	4.2(3)
C(23)	0.3359(10)	−0.351(1)	0.7687(7)	5.4(3)
C(24)	0.423(1)	−0.326(1)	0.7725(8)	6.6(4)
C(25)	0.4610(9)	−0.208(2)	0.7953(9)	7.7(5)
C(26)	0.4076(8)	−0.112(1)	0.8112(7)	5.3(3)
C(27)	0.520(1)	0.479(2)	0.949(1)	5.0(4)

[2.6982(6) Å] and the Mo–Ir vectors [2.8146(9)–2.8222(9) Å] are within the expected ranges. The core carbons C(19) and C(20) interact more closely with iridium [C–Ir 2.074(8), 2.107(9) Å] than with molybdenum [C–Mo 2.290(8)–2.340(8) Å]. All molybdenum-iridium bonds are spanned by a bridging carbonyl ligand. The bridging carbonyls are somewhat asymmetrically disposed [Mo–C 1.98(1)–2.00(1) Å compared to Ir–C 2.314(9)–2.37(1) Å]. It is also noticeable that the Mo–C–O angles for these carbonyls are in the range 153.7(8)–156.7(10)° (a moderate deviation from linearity, as symmetrically bridging carbonyls would have Mo–C–O angles around 135°). These CO ligands are borderline semi-bridging, with asymmetry parameters in the range $\alpha = 0.157$–0.191 [4,5]. The terminal carbonyls are unexceptional, with ∠Ir–C–O angles of 176(1)–179(1)°. Employing the PSEPT (Wade–Mingos Rules), 10 has $\frac{1}{2}$[2 × 6(Mo) + 2 × 9(Ir) + 2 × 5(Cp) + 8 × 2(CO) + 2 × 5(CR)–4 × 12(M)–2 × 2(C)]=7 bonding pairs, electron precise for a *closo*-octahedron.

2.6. Trends in alkyne reactivity

A range of internal and terminal alkynes have thus been shown to react with 1 under mild conditions to

Table 5
Selected bond lengths (Å) and angles (°) for 10

|			
Ir(1)–Ir(2)	2.6982(6)	Ir(2)–C(3)	1.92(1)
Ir(1)–Mo(1)	2.8199(9)	Ir(2)–C(4)	1.93(1)
Ir(1)–Mo(2)	2.8146(9)	Mo(1)–C(9)	2.28(1)
Ir(2)–Mo(1)	2.8209(9)	Mo(1)–C(10)	2.28(1)
Ir(2)–Mo(2)	2.8222(9)	Mo(1)–C(11)	2.32(1)
Ir(1)–C(19)	2.074(8)	Mo(1)–C(12)	2.334(10)
Ir(2)–C(20)	2.107(9)	Mo(1)–C(13)	2.313(10)
Mo(1)–C(19)	2.299(8)	Mo(2)–C(14)	2.29(1)
Mo(1)–C(20)	2.298(8)	Mo(2)–C(15)	2.32(1)
Mo(2)–C(19)	2.290(8)	Mo(2)–C(16)	2.35(1)
Mo(2)–C(20)	2.340(8)	Mo(2)–C(17)	2.33(1)
Ir(1)–C(5)	2.333(9)	Mo(2)–C(18)	2.284(9)
Mo(1)–C(5)	1.98(1)	C(1)–O(1)	1.14(1)
Ir(1)–C(6)	2.314(9)	C(2)–O(2)	1.13(1)
Mo(2)–C(6)	2.00(1)	C(3)–O(3)	1.13(1)
Ir(2)–C(7)	2.35(1)	C(4)–O(4)	1.13(1)
Mo(1)–C(7)	1.98(1)	C(5)–O(5)	1.17(1)
Ir(2)–C(8)	2.37(1)	C(6)–O(6)	1.17(1)
Mo(2)–C(8)	1.99(1)	C(7)–O(7)	1.19(1)
Ir(1)–C(1)	1.91(1)	C(8)–O(8)	1.18(1)
Ir(1)–C(2)	1.91(1)		
Mo(1)–Ir(1)–Mo(2)	95.69(3)	Mo(1)–C(5)–O(5)	155.6(9)
Mo(1)–Ir(2)–Mo(2)	95.50(3)	Ir(1)–C(6)–O(6)	125.1(8)
Mo(1)–Ir(1)–Ir(2)	61.44(2)	Mo(2)–C(6)–O(6)	153.7(8)
Mo(1)–Ir(2)–Ir(1)	61.40(2)	Ir(2)–C(7)–O(7)	123.1(8)
Mo(2)–Ir(1)–Ir(2)	61.54(2)	Mo(1)–C(7)–O(7)	155.9(9)
Mo(2)–Ir(2)–Ir(1)	61.26(2)	Ir(2)–C(8)–O(8)	123.3(9)
Ir(1)–Mo(1)–Ir(2)	57.15(2)	Mo(2)–C(8)–O(8)	156.7(10)
Ir(1)–Mo(2)–Ir(2)	57.20(2)	Ir(1)–C(1)–O(1)	176(1)
Ir(1)–C(19)–C(20)	109.9(6)	Ir(1)–C(2)–O(2)	179(10)
Ir(2)–C(20)–C(19)	105.2(6)	Ir(2)–C(3)–O(3)	176(1)
Ir(2)–Ir(1)–C(19)	71.9(2)	Ir(2)–C(4)–O(4)	177(1)
Ir(1)–Ir(2)–C(20)	73.0(3)	C(19)–C(20)–C(21)	122.5(8)
Ir(1)–C(5)–O(5)	123.2(9)	Ir(2)–C(20)–C(21)	132.3(7)
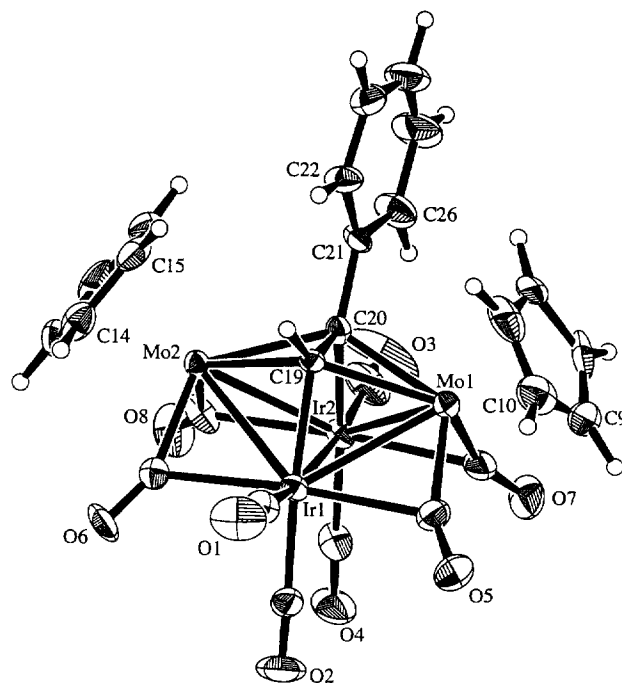
Fig. 3. Molecular structure and atomic labelling scheme for 10. Thermal envelopes of 50% probability are shown for the non-hydrogen atoms; hydrogen atoms have arbitrary radii of 0.1 Å.

afford tetranuclear clusters having the general formula $Cp_2Mo_2Ir_2(\mu_4$-η^2-$RC_2R')(CO)_8$ as the major (and sometimes sole) product in fair to excellent yields (34–80%). These compounds result from the formal insertion of the alkyne into the Mo–Mo bond. The studies with alkynes summarized in Scheme 2 demonstrate two reactivity trends for $Cp_2Mo_2Ir_2(CO)_{10}$ (1). Internal alkynes are less reactive than terminal alkynes which in turn are less reactive than acetylene. Reaction of diphenylacetylene required heating (refluxing dichloromethane) to proceed whereas phenylacetylene reacted at room temperature, although slowly (64 h). In contrast, acetylene reacted rapidly with 1 (2 h) at room temperature to give a mixture of products. Confirmation of this reactivity trend is provided by the reaction of 4,4'-HC≡CC₆H₄C≡CC₆H₄NO₂ (which incorporates both internal and terminal alkyne functionality) with 1, which afforded a product in which the terminal C≡C group had reacted exclusively. A second trend that is observed is that the presence of a nitro group enhances the reactivity of the alkyne over that of the non-nitro analogue. While the reaction of phenylacetylene with 1 required 64 h for complete consumption of the starting cluster, 4-nitrophenylacetylene required only 20 h, and the product was isolated in slightly higher yield. The alkyne chemistry of 1 is thus dependent on steric and electronic effects. The former are clearly important, demonstrated by the reactivity sequence HC≡CH > RC≡CH > RC≡CR. The latter is exemplified by the rate enhancement which occurs upon introduction of an

acceptor group. Although it could be argued that the former is explicable by the electron donating series $H < R$, i.e. by electronic effects, exclusive reaction at the terminal alkyne linkage in 4,4′-$HC\equiv CC_6H_4C\equiv CC_6H_4NO_2$ clearly confirms the importance of steric factors.

The tungsten–iridium cluster $Cp_2W_2Ir_2(CO)_{10}$ (4) underwent addition of diphenylacetylene in refluxing dichloromethane [7] to afford both a complex of the intact alkyne, $Cp_2W_2Ir_2(\mu_4-\eta^2-PhC_2Ph)(CO)_8$ (34%), and a complex $Cp_2W_2Ir_2(\mu_3-CPh)(\mu_3-\eta^3-C_3Ph_3)(CO)_8$ (16%), resulting from cleavage of a W–Ir bond. An analogue of the latter was not observed with 1. Reaction of 4 with the terminal alkyne HC_2Ph at 50°C (1 h) afforded $Cp_2W_2Ir_2(\mu_4-\eta^2-HC_2Ph)(CO)_8$ in excellent yield (80%) [8]. The reaction of HC_2Ph with $Cp_2W_2Co_2(CO)_{10}$ at 55–60°C (24 h) led to a 1:1 addition product isostructural with 9–14 (7%); also formed in this reaction was a mixture of the alkyne oligomerization products 1-, 2-, 4- and 1-, 3-, 5-triphenylbenzene. A comparison of 1 with that of the other metal combinations is clearly of interest. The reactions of excess diphenylacetylene with 1 and 4 both proceeded in refluxing dichloromethane but the product distribution varied. The metal–metal bonds in the tungsten–iridium ($5d$–$5d$) cluster 4 are similar in strength and products resulting from cleavage of a W–W bond and a W–Ir bond were observed [9]. In the case of 1 ($4d$–$5d$), the Mo–Mo bond is substantially weaker than the Mo–Ir and Ir–Ir bonds and only one of the reaction possibilities observed in the tungsten–iridium case was observed (it should be emphasized that the IR spectral data for the minor or trace products obtained in the syntheses of 9–14 are dissimilar to those of the W–Ir cleavage products mentioned above). Likewise, reaction of phenylacetylene with 1 proceeded under milder conditions (room temperature) relative to that with 4 (50°C). Results thus far are consistent with enhanced reactivity in proceeding from tungsten–iridium to molybdenum–iridium clusters, and demonstrate the potential for controlling product distribution in reactions of clusters by selectively weakening specific metal–metal bonds. Further studies are currently under way.

3. Experimental details

Reactions were performed under an atmosphere of argon (high-purity, CIG) with the use of standard Schlenk techniques. No special precautions were taken to exclude air during work-up. The products were purified by thin-layer chromatography on 20 × 20 cm glass plates coated with Merck GF_{254} silica gel (0.5 mm). Thin-layer chromatography used for monitoring the extent of reactions was carried out on plastic sheets coated

with 0.25 mm silica gel with fluorescent indicator (Polygram SIL G/UV_{254}).

The starting cluster $Cp_2Mo_2Ir_2(CO)_{10}$ (1) was prepared by a literature procedure [2]. The reagents PPh_3, PMe_3 (1.0 M in THF), diphenylacetylene and phenylacetylene were purchased commercially (Aldrich) and used as received, while propargyl bromide (Fluka) was distilled twice before use. Acetylene gas (industrial grade, CIG) was passed through two solutions of concentrated H_2SO_4 prior to use. The acetylenes 4-$HC\equiv CC_6H_4NO_2$ and 4,4′-$HC\equiv CC_6H_4C\equiv CC_6H_4NO_2$ were prepared by literature methods [10,11]. THF and n-hexane were laboratory reagent (LR) grade; all other reaction solvents used were analytical reagent (AR) grade. The reaction solvents were dried and distilled under nitrogen using standard methods: CH_2Cl_2 over CaH_2, and THF over sodium benzophenone ketyl. Petroleum spirit refers to a petroleum fraction of boiling range 60–80°C.

Infrared spectra were recorded on a Perkin–Elmer System 2000 FT–IR utilizing a 0.1 mm path length cell with CaF_2 windows; spectral frequencies are recorded in cm^{-1}. All analytical spectra were recorded as solutions in either cyclohexane or CH_2Cl_2 (both AR grade). ^1H or room temperature ^{31}P-NMR spectra were recorded in $CDCl_3$ (Cambridge Isotope Laboratories) using a Varian Gemini-300 spectrometer (^1H at 300 MHz, ^{31}P at 121 MHz) and are referenced to residual $CHCl_3$ (7.24 ppm) or external 85% H_3PO_4 (0.00 ppm), respectively. Variable temperature (230 K) ^{31}P-NMR spectra were recorded in $CDCl_3$ (CIL) using a Varian VXR300S spectrometer (at 121 MHz) and are referenced to external 85% H_3PO_4 (0.00 ppm). Mass spectra were recorded using a VG ZAB 2SEQ instrument (30 kV Cs^+ ions, current 1 mA, accelerating potential 8 kV, 3-nitrobenzyl alcohol matrix) at the Research School of Chemistry, Australian National University; peaks are reported as m/z (assignment, relative intensity). Elemental microanalyses were carried out by the Microanalysis Service Unit in the Research School of Chemistry, Australian National University.

3.1. Reaction of $Cp_2Mo_2Ir_2(CO)_{10}$ with 1 equivalent of PPh_3

A red-brown solution of $Cp_2Mo_2Ir_2(CO)_{10}$ (1) (34.1 mg, 0.0346 mmol) and PPh_3 (9.1 mg, 0.035 mmol) in CH_2Cl_2 (30 ml) was stirred at room temperature for 24 h. The dark red-brown solution obtained was evaporated to dryness on a rotary evaporator, and then the residue dissolved in CH_2Cl_2 (ca. 3 ml) and applied to preparative TLC plates. Elution with CH_2Cl_2/petroleum spirit (3/2) gave three bands.

The contents of the first band, $R_f = 0.60$, were identified by solution IR as unreacted $Cp_2Mo_2Ir_2(CO)_{10}$ (1) (2.2 mg, 0.0022 mmol (6%)).

The second and major band, $R_f = 0.46$, was crystallized from $CH_2Cl_2/MeOH$ at 3°C to afford dark red-brown crystals of $Cp_2Mo_2Ir_2(CO)_9(PPh_3)$ (5) (25.3 mg, 0.0207 mmol (60%)).

The third band, $R_f = 0.26$, was identified as $Cp_2Mo_2Ir_2(CO)_8(PPh_3)_2$ (6) (2.5 mg, 0.0017 mmol (5%)) by comparison of its solution IR spectrum with that of an authentic sample (see below).

3.2. Reaction of $Cp_2Mo_2Ir_2(CO)_{10}$ with 2 equivalents of PPh_3

Following the method for Section 3.1, $Cp_2Mo_2Ir_2(CO)_{10}$ (1) (38.6 mg, 0.0391 mmol) was reacted with PPh_3 (20.5 mg, 0.0782 mmol) at room temperature for 24 h. Purification by preparative chromatography with $CH_2Cl_2/petroleum$ spirit (3/2) eluent gave two bands.

The first band, $R_f = 0.44$, was identified by solution IR as $Cp_2Mo_2Ir_2(CO)_9(PPh_3)$ (5) (9.6 mg, 0.0078 mmol (20%)).

The second band, $R_f = 0.25$, was found to decompose slowly during development of the chromatography plate. Solution IR and ^1H-NMR spectra indicated that the band contained primarily $Cp_2Mo_2Ir_2(CO)_8(PPh_3)_2$ (20.5 mg, 0.0141 mmol (36%)) (6), but also a small quantity of $Cp_2Mo_2Ir_2(CO)_9(PPh_3)$ (5). The contents of the second band were crystallized from $CHCl_3/petroleum$ spirit at 3°C to afford dark red-brown crystals. Purification attempts failed to isolate 6 without contamination.

3.3. Analytical data for 5 and 6

5: Anal. Found: C, 36.52; H, 2.14%. $C_{37}H_{25}Ir_2Mo_2O_9P$ Calcd.: C, 36.40; H, 2.06%. IR $(c-C_6H_{12})$: $\nu(CO)$ 2063w, 2043s, 2026m, 2005m, 1989vs, 1982s, 1966sh, 1961m, 1932sh, 1924m, 1875m, 1839m, 1815w, 1780w, 1760m, 1743m cm^{-1}. ^1H-NMR $(CDCl_3)$: δ 7.47–7.25 (m, 15H, Ph), 4.66 (s, 10H, Cp) ppm. ^{31}P-NMR $(CDCl_3, 230 K)$: 14.9 (s, 0.33P), 3.2 (s, 0.67P) ppm. MS: 1220 ([M]$^+$, 14), 1992 ([M–CO]$^+$, 84), 1164 ([M–2CO]$^+$, 89), 1136 ([M–3CO]$^+$, 36), 1108 ([M–4CO]$^+$, 68), 1080 ([M–5CO]$^+$, 76), 1052 ([M–6CO]$^+$, 44), 1024 ([M–7CO]$^+$, 100), 996 ([M–8CO]$^+$, 64), 968 ([M–9CO]$^+$, 74), 931 ([M–CO–PPh_3]$^+$, 26), 919 ([M–8CO–Ph]$^+$, 42), 902 ([M–2CO–PPh_3]$^+$, 42), 891 ([M–9CO–Ph]$^+$, 87.

6: IR $(c-C_6H_{12})$: $\nu(CO)$ 1999s, 1981s, 1950vs(br), 1903s(br), 1848m(br), 1800m, 1773m, 1734s cm^{-1}. ^1H-NMR $(CDCl_3)$: δ 7.58–7.20 (m, 30H, Ph), 4.40 (s (br), 10H, Cp) ppm. ^{31}P-NMR $(CDCl_3, 230K)$: 18.4 (s, 1P), 13.5 (s, 1P) ppm. MS: 1456 ([M]$^+$, 57), 1428 ([M–CO]$^+$, 10), 1400 ([M–2CO]$^+$, 78), 1323 ([M–2CO–Ph]$^+$, 6), 1211 ([M–6CO–Ph]$^+$, 33), 1194 ([M–PPh_3]$^+$, 23), 1166 ([M–CO–PPh_3]$^+$, 57), 1138 ([M–2CO–PPh_3]$^+$, 23), 1110 ([M–3CO–PPh_3]$^+$, 49), 1082 ([M–4CO–PPh_3]$^+$, 63), 1054 ([M–5CO–PPh_3]$^+$, 31), 1026 ([M–6CO–PPh_3]$^+$, 77), 998 ([M–7CO–PPh_3]$^+$, 100), 970 ([M–8CO–PPh_3]$^+$, 49), 921 ([M–7CO–PPh_3–Ph]$^+$, 43), 893 ([M–8CO–PPh_3–Ph]$^+$, 65).

3.4. Reaction of $Cp_2Mo_2Ir_2(CO)_{10}$ with 1 equivalent of PMe_3

A red-brown solution of $Cp_2Mo_2Ir_2(CO)_{10}$ (1) (26.5 mg, 0.0268 mmol) and PMe_3 (27 μl, 1 M solution in THF, 0.027 mmol) in THF (30 ml) was stirred at room temperature for 24 h. The dark red-brown solution obtained was evaporated to dryness on a rotary evaporator, and then the residue dissolved in CH_2Cl_2 (ca. 3 ml) and applied to preparative TLC plates. Elution with $CH_2Cl_2/petroleum$ spirit (3/2) gave three bands.

The contents of the first band, $R_f = 0.61$, were identified by solution IR as unreacted $Cp_2Mo_2Ir_2(CO)_{10}$ (1) (4.5 mg, 0.0046 mmol (17%)).

The second and major band, $R_f = 0.38$, was crystallized from CH_2Cl_2/n-hexane at 3°C to afford dark red-brown crystals of $Cp_2Mo_2Ir_2(CO)_9(PMe_3)$ (7) (11.1 mg, 0.0107 mmol (40%)).

The third band, $R_f = 0.15$, was recrystallized from CH_2Cl_2/n-hexane at 3 °C to afford dark red-brown crystals of $Cp_2Mo_2Ir_2(CO)_8(PMe_3)_2$ (8) (9.0 mg, 0.0083 mmol (31%)).

3.5. Reaction of $Cp_2Mo_2Ir_2(CO)_{10}$ with 2 equivalents of PMe_3

Following the method for Section 3.4, $Cp_2Mo_2Ir_2(CO)_{10}$ (1) (38.7 mg, 0.0392 mmol) was reacted with PMe_3 (79 μl, 1 M solution in THF, 0.079 mmol) at room temperature for 24 h. Purification by preparative chromatography with $CH_2Cl_2/petroleum$ spirit (3/2) eluent gave two bands.

The first band, $R_f = 0.40$, in trace amounts, was identified by solution IR as $Cp_2Mo_2Ir_2(CO)_9(PMe_3)$ (7).

The second and major band, $R_f = 0.17$, was identified by solution IR as $Cp_2Mo_2Ir_2(CO)_8(PMe_3)_2$ (33.2 mg, 0.0307 mmol (78%)) (8).

3.6. Reaction of $Cp_2Mo_2Ir_2(CO)_{10}$ with excess PMe_3

Following the method for Section 3.4, $Cp_2Mo_2Ir_2(CO)_{10}$ (1) (22.8 mg, 0.0231 mmol) was reacted with PMe_3 (116 μl, 1 M solution in THF, 0.116 mmol) at room temperature for 24 h. Purification by preparative chromatography with $CH_2Cl_2/petroleum$ spirit (3/2) eluent gave one band. The sole product, $R_f = 0.16$, was identified by solution IR as $Cp_2Mo_2Ir_2(CO)_8(PMe_3)_2$ (20.2 mg, 0.0187 mmol (81%)) (8).

3.7. Analytical data for 7 and 8

7: Anal. Found: C, 25.47; H, 1.59%. $C_{22}H_{19}Ir_2Mo_2O_9P$ Calcd.: C, 25.54; H, 1.85%. IR (c-C_6H_{12}): ν(CO) 2043w, 2030vs, 2002s, 1989vs, 1975vs, 1969m, 1964m, 1926m, 1900w, 1809w, 1868m, 1856sh, 1833m, 1779m, 1756s cm^{-1}. ^{1}H-NMR (CDCl$_3$): δ 4.86 (s, 10H, Cp), 1.86 (d, J(HP) = 17 Hz, 9H, Me) ppm. ^{31}P-NMR (CDCl$_3$, 230 K): −21.9 (s), −22.8 (s (br)) ppm. MS: 1034 ([M]$^+$, 6), 1006 ([M−CO]$^+$, 18), 978 ([M−2CO]$^+$, 47), 950 ([M−3CO]$^+$, 50), 922 ([M−4CO]$^+$, 38), 894 ([M−5CO]$^+$, 100), 866 ([M−6CO]$^+$, 55), 838 ([M−7CO]$^+$, 67), 808 ([M−7CO−2Me]$^+$, 35), 790 ([M−6CO−PMe$_3$]$^+$, 22), 780 ([M−8CO−2Me]$^+$, 28), 762 ([M−7CO−PMe$_3$]$^+$, 30), 752 ([M−9CO−2Me]$^+$, 12), 734 ([M−8CO−PMe$_3$]$^+$, 11), 725 ([M−6CO−PMe$_3$−Cp]$^+$, 6), 706 ([M−9CO−PMe$_3$]$^+$, 10), 697 ([M−7CO−PMe$_3$−Cp]$^+$, 5).

8: Anal. Found: C, 26.43; H, 2.43%. $C_{24}H_{28}Ir_2Mo_2O_8P_2$ Calcd.: C, 26.62; H, 2.61%. IR (c-C_6H_{12}): ν(CO) 2015w, 1994w, 1985m, 1974s, 1961vs, 1945s, 1903w, 1870m(br), 1838m, 1814sh, 1805m, 1763m, 1739s cm^{-1}. ^{1}H-NMR (CDCl$_3$): δ 4.79 (s, br), 10H, Cp), 1.81 (d, J(HP) = 10 Hz, 18H, Me) ppm. ^{31}P-NMR (CDCl$_3$, 230 K): −17.2 (s (br), 0.8P), −22.0 (s, 0.2P), −27.0 (s, 0.2P), −34.3 (s (br), 0.8P) ppm. ^{31}P-NMR (CDCl$_3$, 213 K): −17.0 (s, 1P), −22.6 (s, 1P), −26.5 (s, 1P), −33.7 (s, 1P) ppm. MS: 1054 ([M−CO]$^+$, 20), 1026 ([M−2CO]$^+$, 51), 998 ([M−3CO]$^+$, 42), 970 ([M−4CO]$^+$, 50), 942 ([M−5CO]$^+$, 100), 914 ([M−6CO]$^+$, 65), 894 ([M−4CO−PMe$_3$]$^+$, 21), 884 ([M−6CO−2Me]$^+$, 45), 866 ([M−5CO−PMe$_3$]$^+$, 35), 851 ([M−5CO−PMe$_3$−Me]$^+$, 42), 838 ([M−6CO−PMe$_3$]$^+$, 55), 823 ([M−6CO−PMe$_3$−Me]$^+$, 32), 808 ([M−6CO−PMe$_3$−2Me]$^+$, 77), 790 ([M−5CO−2PMe$_3$]$^+$, 34), 780 ([M−7CO−PMe$_3$−2Me]$^+$, 33), 762 ([M−6CO−2PMe$_3$]$^+$, 29), 753 ([M−4CO−2PMe$_3$−Cp]$^+$, 31), 734 ([M−7CO−2PMe$_3$]$^+$, 16), 725 ([M−5CO−2PMe$_3$−Cp]$^+$, 27), 706 ([M−8CO−2PMe$_3$]$^+$, 23).

3.8. Reaction of $Cp_2Mo_2Ir_2(CO)_{10}$ with diphenylacetylene (PhC≡CPh)

Diphenylacetylene (27.6 mg, 0.155 mmol) was added to a red-brown solution of $Cp_2Mo_2Ir_2(CO)_{10}$ (1) (30.0 mg, 0.0304 mmol) in CH$_2$Cl$_2$ (30 ml) and the resultant mixture stirred at reflux for 23 h, over which time the colour changed to dark green. The solution was then taken to dryness on a rotary evaporator, and then the residue dissolved in a minimum of CH$_2$Cl$_2$ (ca. 3 ml) and applied to preparative chromatography plates. Elution with CH$_2$Cl$_2$/petroleum spirit (3/2) gave two bands. The second band, R_f = 0.48, was crystallized from CH$_2$Cl$_2$/MeOH at −18°C to afford dark green microcrystals of $Cp_2Mo_2Ir_2(\mu_4$-η^2-PhC$_2$Ph)(CO)$_8$ (9) (26.9 mg, 0.0243 mmol (80%)). Anal. Found: C, 34.39; H, 1.57%. $C_{32}H_{20}Ir_2Mo_2O_8$ Calcd.: C, 34.66; H,

1.82%. IR (CH$_2$Cl$_2$): ν(CO) 2071vs, 2046vs, 2021m, 2001m, 1813s, 1772sh, 1760m cm^{-1}. ^{1}H-NMR (CDCl$_3$): δ 7.18–7.02 (m, 10H, Ph), 4.77 (s, 10H, Cp) ppm. MS: 1108 ([M]$^+$, 67), 1052 ([M−2CO]$^+$, 100), 1024 ([M−3CO]$^+$, 82), 996 ([M−4CO]$^+$, 57), 968 ([M−5CO]$^+$, 61), 940 ([M−6CO]$^+$, 63), 912 ([M−7CO]$^+$, 56), 884 ([M−8CO]$^+$, 90).

3.9. Reaction of $Cp_2Mo_2Ir_2(CO)_{10}$ with phenylacetylene (HC≡CPh)

Following the procedure of Section 3.8, phenylacetylene (14 μl, 13 mg, 0.13 mmol) was reacted with $Cp_2Mo_2Ir_2(CO)_{10}$ (1) (25.5 mg, 0.0259 mmol) at room temperature for 64 h. Purification by preparative chromatography (multiple developments) with CH$_2$Cl$_2$/petroleum spirit (3/2) eluent gave three bands. The first band, R_f = 0.25, was crystallized from CH$_2$Cl$_2$/MeOH at −18°C to afford dark green microcrystals of $Cp_2Mo_2Ir_2(\mu_4$-η^2-HC$_2$Ph)(CO)$_8$ (10) (16.3 mg, 0.0158 mmol (61%)). Anal. Found: C, 29.68; H, 0.92%. $C_{26}H_{16}Ir_2Mo_2O_8$ Calcd.: C, 30.24; H, 1.56%. IR (CH$_2$Cl$_2$): ν(CO) 2067vs, 2039vs, 2013m, 1994m, 1824s, 1777m cm^{-1}. ^{1}H-NMR (CDCl$_3$): δ 10.22 (s, 1H, CH), 7.3–6.6 (m, 5H, Ph), 4.80 (s, 10H, Cp) ppm. MS: 1033 ([M]$^+$, 42), 977 ([M−2CO]$^+$, 63), 949 ([M−3CO]$^+$, 55), 921 ([M−4CO]$^+$, 65), 893 ([M−5CO]$^+$, 77), 865 ([M−6CO]$^+$, 75), 837 ([M−7CO]$^+$, 68), 809 ([M−8CO]$^+$, 100).

3.10. Reaction of $Cp_2Mo_2Ir_2(CO)_{10}$ with 4-HC≡CC$_6$H$_4$NO$_2$

Following the procedure of Section 3.8, 4-nitrophenylacetylene (15.2 mg, 0.103 mmol) was reacted with $Cp_2Mo_2Ir_2(CO)_{10}$ (1) (20.0 mg, 0.0203 mmol) at room temperature for 20 h. Purification by preparative chromatography with CH$_2$Cl$_2$/petroleum spirit (3/2) eluent gave one band. The sole product, R_f = 0.23, was crystallized by diffusion of n-hexane/acetone (70:30) into CH$_2$Cl$_2$ at −18°C to afford dark green-brown microcrystals of $Cp_2Mo_2Ir_2(\mu_4$-η^2-4-HC$_2$C$_6$H$_4$NO$_2$)(CO)$_8$ (11) (14.0 mg, 0.0130 mmol (64%)). Anal. Found: C, 28.31; H, 1.10; N, 1.46%. $C_{26}H_{15}Ir_2Mo_2NO_{10}$ Calcd.: C, 28.98; H, 1.40; N, 1.30%. IR (CH$_2$Cl$_2$): ν(CO) 2071vs, 2043vs, 2017m, 1998m, 1831m, 1785m cm^{-1}. ^{1}H-NMR (CDCl$_3$): δ 10.08 (s, 1H, CH), 8.1–6.6 (m, 4H, C$_6$H$_4$), 4.84 (s, 10H, Cp) ppm. MS: 1078 ([M]$^+$, 100), 1050 ([M−CO]$^+$, 66), 1022 ([M−2CO]$^+$, 60), 994 ([M−3CO]$^+$, 72), 966 ([M−4CO]$^+$, 90), 938 ([M−5CO]$^+$, 80), 910 ([M−6CO]$^+$, 45), 882 ([M−7CO]$^+$, 37), 854 ([M−8CO]$^+$, 16).

3.11. Reaction of $Cp_2Mo_2Ir_2(CO)_{10}$ with 4,4'-HC≡CC$_6$H$_4$C≡CC$_6$H$_4$NO$_2$

Following the procedure of Section 3.8, 4,4'-HC≡CC$_6$H$_4$C≡CC$_6$H$_4$NO$_2$ (10.0 mg, 0.0404 mmol)

was reacted with $Cp_2Mo_2Ir_2(CO)_{10}$ (1) (20.5 mg, 0.0208 mmol) at room temperature for 50 h. Purification by preparative chromatography with CH_2Cl_2/petroleum spirit (3/2) eluent gave one band. The sole product, $R_f = 0.22$, was crystallized by diffusion of n-hexane/acetone (70:30) into CH_2Cl_2 at $-18°C$ to afford dark green microcrystals of $Cp_2Mo_2Ir_2(\mu_4\text{-}\eta^2\text{-}4,4'\text{-HC}_2C_6H_4C\equiv CC_6H_4NO_2)(CO)_8$ (12) (15.4 mg, 0.0131 mmol (63%)). Anal. Found: C, 34.84; H, 1.45; N, 1.46%. $C_{34}H_{19}Ir_2Mo_2NO_{10}$ Calcd.: C, 34.67; H, 1.63; N, 1.19%. IR (CH_2Cl_2): $\nu(C\equiv C)$ 2217 cm^{-1}; $\nu(CO)$ 2068vs, 2041vs, 2014m, 1996m, 1827s, 1779m cm^{-1}. ^{1}H-NMR $(CDCl_3)$: δ 10.15 (s, 1H, CH), 8.3–6.6 (m, 8H, C_6H_4), 4.84 (s, 10H, Cp) ppm. MS: 1178 ([M]$^+$, 100), 1150 ([M–CO]$^+$, 41), 1122 ([M–2CO]$^+$, 79), 1094 ([M–3CO]$^+$, 36), 1066 ([M–4CO]$^+$, 52), 1038 ([M–5CO]$^+$, 50), 1010 ([M–6CO]$^+$, 24), 982 ([M–7CO]$^+$, 32), 972 ([M–3CO–$C_6H_4NO_2$]$^+$, 30), 954 ([M–8CO]$^+$, 28), 944 ([M–4CO–$C_6H_4NO_2$]$^+$, 32), 916 ([M–5CO–$C_6H_4NO_2$]$^+$, 30), 888 ([M–6CO–$C_6H_4NO_2$]$^+$, 50), 860 ([M–7CO–$C_6H_4NO_2$]$^+$, 38).

3.12. Reaction of $Cp_2Mo_2Ir_2(CO)_{10}$ with $HC\equiv CCH_2Br$

Following the procedure of Section 3.8, $HC\equiv CCH_2Br$ (10 μl, 13 mg, 0.11 mmol) was reacted with $Cp_2Mo_2Ir_2(CO)_{10}$ (1) (20.2 mg, 0.0205 mmol) at room temperature for 20 h. Purification by preparative chromatography with CH_2Cl_2/petroleum spirit (3/1) eluent gave four bands. The fourth and major band, $R_f = 0.08$, was crystallized from CH_2Cl_2/n-hexane at $-18°C$ to afford dark green crystals of $Cp_2Mo_2Ir_2(\mu_4\text{-}\eta^2\text{-HC}_2CH_2Br)(CO)_8$ (13) (7.3 mg, 0.0070 mmol (34%)). Anal. Found: C, 24.53; H, 1.04%. $C_{21}H_{13}BrIr_2Mo_2O_8$ Calcd.: C, 24.03; H, 1.25%. IR (CH_2Cl_2): $\nu(CO)$ 2067s, 2040vs, 2013m, 1995m, 1822m, 1775m cm^{-1}. ^{1}H-NMR $(CDCl_3)$: δ 9.79 (s, 1H, CH), 5.27 (s, 10H, Cp), 3.82 (s, 1H, CH_2), 3.80 (s, 1H, CH_2) ppm. MS: 985 ([M–Cp]$^+$, 76), 957 ([M–Cp–CO]$^+$, 31), 929 ([M–Cp–2CO]$^+$, 77), 901 ([M–Cp–3CO]$^+$, 50), 873 ([M–Cp–4CO]$^+$, 82), 845 ([M–Cp–5CO]$^+$, 100), 817 ([M–Cp–6CO]$^+$, 86), 789 ([M–Cp–7CO]$^+$, 71), 761 ([M–Cp–8CO]$^+$, 75).

3.13. Reaction of $Cp_2Mo_2Ir_2(CO)_{10}$ with $HC\equiv CH$

Acetylene $(HC\equiv CH)$ was bubbled through a stirred red-brown solution of $Cp_2Mo_2Ir_2(CO)_{10}$ (1) (30.9 mg, 0.0313 mmol) in CH_2Cl_2 (40 ml) at room temperature for 2 h. Over this time, the solution changed to green-brown. The resulting solution was taken to dryness on a rotary evaporator, and then the residue dissolved in a minimum of CH_2Cl_2 (ca. 4 ml) and applied to preparative TLC plates. Elution with CH_2Cl_2/petroleum spirit (3/2) gave five bands. The second and major band, $R_f = 0.67$, was extracted with CH_2Cl_2 to give a blue-

green solution. Removal of the solvent and crystallization from CH_2Cl_2/n-hexane at $-18°C$ afforded dark red crystals of $Cp_2Mo_2Ir_2(\mu_4\text{-}\eta^2\text{-HC}_2H)(CO)_8$ (14) (13.2 mg, 0.0138 mmol (44%)). Anal. Found: C, 25.02; H, 1.21%. $C_{20}H_{12}Ir_2Mo_2O_8$ Calcd.: C, 25.11; H, 1.26%. IR (CH_2Cl_2): $\nu(CO)$ 2065s, 2038vs, 2012m, 1992m, 1825m, 1780m cm^{-1}. ^{1}H-NMR $(CDCl_3)$: δ 9.23 (s, 2H, CH), 5.31 (s, 10H, Cp) ppm. MS: 957 ([M]$^+$, 55), 929 ([M–CO]$^+$, 60), 901 ([M–2CO]$^+$, 75), 873 ([M–3CO]$^+$, 70), 845 ([M–4CO]$^+$, 85), 817 ([M–5CO]$^+$, 90), 789 ([M–6CO]$^+$, 100), 761 ([M–7CO]$^+$, 90), 733 ([M–8CO]$^+$, 70).

3.14. X-ray structure determinations

3.14.1. Experimental conditions

Crystals of complexes 7a and 10 were grown by liquid diffusion from CH_2Cl_2/n-hexane and CH_2Cl_2/MeOH, respectively, at 3°C. Unique diffractometer data sets were collected on a Rigaku AFC7R diffractometer at 295 K within the $2\theta_{max}$ limit 50° (ω-2θ scan mode; monochromatic Mo K_α radiation ($\lambda = 0.71069$ Å)) yielding 4500 (7a) and 5143 (10) independent reflections. 3028 of these with $I > 3.5\sigma(I)$ (7a) and 3361 of these with $I > 3.00\sigma(I)$ (10) were considered 'observed' and used in the full-matrix least squares refinement after Lorentz-polarization, empirical absorption (transmission factors 0.60–1.00 (7a) or 0.39–1.00 (10)) and secondary extinction corrections. Anisotropic thermal parameters were refined for some non-hydrogen atoms, while the rest were refined isotropically; $(x, y, z, U_{iso})_H$ were included, constrained at estimated values. A disordered dichloromethane solvent molecule was modeled as 0.7 site occupancy. Conventional residuals R, R_w on $|F|$ at convergence are given, the weighting function $w = 4F_0^2/\sigma^2(F_0^2)$ where $\sigma^2(F_0^2) = [S^2(C + R^2B) + (pF_0^2)^2]/Lp^2$ (S = scan rate, C = peak count, R = ratio of scan time to background counting time, B = background count, $p = 0.0060$ (7a) or 0.0070 (10) determined experimentally from standard reflections) being employed. Computation used the teXsan package [12]. Pertinent results are given in the figures and tables. Tables of hydrogen atom coordinates and thermal parameters and complete lists of bond lengths and angles for non-hydrogen atoms have been deposited at the Cambridge Crystallographic Data Centre.

3.14.2. Crystal data for 7a and 10

7a: $C_{22}H_{19}Ir_2Mo_2O_9P$, $M = 1034.68$. Triclinic, space group $P\bar{1}$(No. 2), $a = 9.847(4)$, $b = 14.78(2)$, $c = 8.870(4)$ Å, $\alpha = 91.72(6)$, $\beta = 99.17(4)$, $\gamma = 93.63(6)°$, $V = 1270(1)$ Å^3, $Z = 2$. $D_{calc} = 2.704$ g cm^{-3}; $F(000) = 952$. $\mu_{Mo} = 115.42$ cm^{-1}; specimen: 0.10 × 0.10 × 0.20 mm^3; $T_{min, max} = 0.60, 1.00$; $R = 0.043$; $R_w = 0.045$.

10: $C_{26.70}H_{16}ClIr_2Mo_2O_8$, $M = 1068.18$. Monoclinic, space group $P2_1/c$ (No. 14), $a = 15.327(2)$, $b = 10.479(2)$, $c = 17.830(1)$ Å, $\beta = 105.633(7)°$, $V = 2757.8(6)$ Å^3, $Z = 4$. $D_{calc} = 2.572$ g cm^{-3}; $F(000) = 1964$. $\mu_{Mo} = 106.78$ cm^{-1}; specimen: $0.35 \times 0.20 \times 0.10$ mm^3; $T_{min, max} = 0.39$, 1.00; $R = 0.027$; $R_w = 0.027$.

Acknowledgements

References

[1] N.T. Lucas, I.R. Whittall, M.G. Humphrey, D.C.R. Hockless, M.P.S. Perera, M.L. Williams, J. Organomet. Chem. 540 (1997) 147.

[2] N.T. Lucas, M.G. Humphrey, D.C.R. Hockless, J. Organomet. Chem. 535 (1997) 175.

[3] C. Barnes, in E.W. Abel, F.G.A. Stone, G. Wilkinson (Eds.), Comprehensive Organometallic Chemistry II, Vol. 8, Pergamon, Oxford, 1996, p. 490.

[4] M.D. Curtis, W.M. Butler, J. Organomet. Chem. 155 (1978) 131.

[5] R.J. Klingler, W.M. Butler, M.D. Curtis, J. Am. Chem. Soc. 100 (1978) 5034.

[6] S.M. Waterman, M.G. Humphrey, V.-A. Tolhurst, B.W. Skelton, A.H. White, D.C.R. Hockless, Organometallics 15 (1996) 934.

[7] J.R. Shapley, C.H. McAteer, M.R. Churchill, L.V. Biondi, Organometallics 3 (1984) 1595.

[8] V.-A. Tolhurst, Honours Thesis, University of New England, Australia, 1993.

[9] J.R. Shapley, M.G. Humphrey, C.H. McAteer, in: M.E. Davis, S.L. Suib (Eds.), ACS Symposium Series Vol. 517, Selectivity in Catalysis, American Chemical Society, New York, 1993, p. 127.

[10] S. Takahashi, Y. Kuroyama, K. Sonogashira, N. Hagihara, Synthesis (1980) 627.

[11] I.R. Whittall, M.P. Cifuentes, M.G. Humphrey, B. Luther-Davies, M. Samoc, S. Houbrechts, A. Persoons, G.A. Heath, D.C.R. Hockless, J. Organomet. Chem. (1997) in press.

[12] teXsan; Single Crystal Structure Analysis Software, Version 1.6c, Molecular Structure Corporation, The Woodlands, TX, 1993.